DOI: 10.1002/adma.200601618

Dual Nanoparticle/Substrate Control of Catalytic Dehydrogenation**

By *Albina Y. Borisevich*,* *Sanwu Wang*, *Sergey N. Rashkeev*, *Michael Glazoff*, *Stephen J. Pennycook*, and *Sokrates T. Pantelides*

Saturated hydrocarbons, or alkanes (C_nH_{2n+2}), are abundant in petroleum and can be converted to alkenes (C_nH_{2n}) by dehydrogenation. Alkenes, also known as unsaturated hydrocarbons, are easy to polymerize and are the primary feedstock of the petrochemical industry, especially ethene ($n = 2$) and propene ($n = 3$).[1,2] Efficient catalytic dehydrogenation is therefore a major industrial objective. It has been found that oxidative catalytic dehydrogenation, that is, a process assisted by both a solid catalyst and a flow of oxygen gas, is most practical because of higher system longevity.[3–5] Chromia/alumina catalytic systems have been widely adopted by industry. They have also been the subject of scientific studies seeking understanding that may help optimization of the process.[3,4,6,7]

It has been established that the catalytic activity of chromia/alumina catalysts first increases with chromia loading, but then starts to decrease.[3,5] Degradation at higher coverages has been correlated with the appearance of crystalline Cr_2O_3 particles. Thus far, characterization of the low-loading regime has been pursued with a variety of techniques, all of which probe relatively large surface areas, yielding an average signal.[3,5,8,9] It has been inferred that "surface chromate species", as opposed to fragments of stoichiometric oxides, are responsible for catalysis. Efforts to determine the oxidation state of Cr in catalytically active species have yielded conflicting results, but a consensus has emerged that Cr^{6+} is present. Further identification of the species, the local coordination of Cr and O atoms, and details of the catalytic reactions at the atomic level have remained elusive. In addition, it has recently been established that there are major disparities in catalyst behavior when different alumina polytypes are used as supports. Among the so-called transition aluminas, all of which are porous and have a cubic spinel structure,[10,11] chromia on η-alumina is a highly active catalyst with a lifetime of several years, whereas the activity of chromia on γ-alumina degrades within weeks.[12,13] Differences between the surfaces of these two polytypes are well-known and have been attributed to different reconstructions, controlled by the different distributions of bulk Al vacancies.[14] Prior theoretical work[15] found that single Cr atoms adsorb stably on η-alumina surfaces but get buried in the subsurface layers on γ-alumina surfaces. The effect was proposed as a possible mechanism for the observed rapid degradation of γ-alumina/chromia catalyst systems.

In this Communication we combine several experimental techniques and first-principles quantum-mechanical calculations to provide atomic-scale understanding of alumina/chromia systems, the oxidative dehydrogenation of alkanes, and the nanoparticle–substrate interactions that control catalytic activity. More specifically, we used direct imaging by *Z*-contrast aberration-corrected scanning transmission electron microscopy (STEM) and electron energy loss spectroscopy (EELS) coupled with extended X-ray absorption fine structure (EXAFS) measurements. In contrast to prior techniques, whose probes cover relatively large surface areas, the STEM electron beam is focused in sub-Ångstrom regions, and is scanned so that the *Z*-contrast images and EELS measurements provide information with atomic resolution. We use these techniques to demonstrate that chromia on η-alumina appears in monodisperse form, predominantly as CrO_x clusters. We further demonstrate that such clusters remain mono-

[*] A. Y. Borisevich, S. N. Rashkeev,[+] S. J. Pennycook, S. T. Pantelides
Materials Science and Technology Division
Oak Ridge National Laboratory
Oak Ridge, TN 37831 (USA)
E-mail: albinab@ornl.gov

S. Wang
Department of Physics and Engineering Physics
University of Tulsa
Tulsa, OK 74104 (USA)

S. Wang, S. N. Rashkeev,[+] S. J. Pennycook, S. T. Pantelides
Department of Physics and Astronomy
Vanderbilt University
Nashville, TN 37235 (USA)

M. Glazoff
Alcoa Technical Center
Alcoa Center, PA 15069 (USA)

[+] Present address: Idaho National Laboratory, Center for Advanced Modeling and Simulation, Idaho Falls, ID 83415-2208, USA.

[**] This work was supported in part by the National Science Foundation Grant DMR-0111841, by the William A. and Nancy F. McMinn Endowment at Vanderbilt University, by the Division of Materials Sciences and Engineering, Office of Basic Energy Sciences, U.S. Department of Energy, under contract DE-AC05-00OR22725 with Oak Ridge National Laboratory, managed and operated by UT-Battelle, LLC, and by an appointment to the RNL Postdoctoral Research Program administered jointly by ORNL and Oak Ridge Institute for Science and Education (ORISE). Access to the Novosibirsk Synchrotron Facility of the Russian Academy of Sciences and to the supercomputers at Florida State University and at ORNL is acknowledged. This work was also supported in part by a grant of computer time from the DoD High Performance Computing Modernization Program at the Maui High Performance Computer Center (MHPCC). We thank Dr. Saeed Alerasool and Dr. Michael Breen, BASF Catalysts, for providing catalyst samples.

© 2007 WILEY-VCH Verlag GmbH & Co. KGaA, Weinheim

ADVANCED MATERIALS

disperse after annealing, with no evidence of agglomeration. In contrast, agglomeration occurs on γ-alumina, leading to Cr_2O_3 patches. Our theoretical calculations suggest that CrO_x clusters adsorbed on either γ- or η-alumina are catalytically active. The key active sites are low-coordination-number O atoms on the CrO_x clusters that are able to strip H atoms from alkanes. Flowing O_2 molecules then strip the H atoms from the catalyst to form H_2O molecules, allowing the process to reiterate. In contrast, we find that crystalline Cr_2O_3 surfaces, where O atoms have higher coordination numbers, do not mediate the catalytic reaction (the transfer of H atoms from the alkanes to the surface O atoms costs energy). Finally, we show that the catalytically active CrO_x clusters adsorb stably on both γ- and η-alumina surfaces, but that degradation of the γ-alumina/chromia systems occurs because reconstruction on γ-alumina facilitates the formation of crystalline Cr_2O_3 *in registry with the substrate*, while the reconstruction on η-alumina does not.

Z-contrast STEM studies demonstrate a marked difference in the Cr distribution on γ- and η-Al_2O_3. For γ-Al_2O_3 at high loadings of Cr the distribution is highly nonuniform, as illustrated by a *Z*-contrast image of the sample with ca. 2.5 monolayer (ML) loading in Figure 1a. In this imaging mode, the intensity contributed by an atom is roughly proportional to Z^2, where Z is the atomic number,[16] so that Cr-rich regions ($Z_{Cr} = 24$) appear bright on the background of the alumina support ($Z_{Al} = 13$). Cr is visibly segregated into extended "patches" on the γ-alumina surface. The chemical nature of the contrast is confirmed by EELS studies (Fig. 1b), which show a strong Cr signal on the patches and no detectable Cr signal between the patches. Diffractograms of the images of the patches contain Cr_2O_3 reflections; moreover, Cr_2O_3 lattice spacings can also be identified in a conventional powder X-ray diffraction pattern along with alumina reflections, which is consistent with the observed patch size of several nanometers. Overall, bright patches of chromia can be found on samples with both above-monolayer (Fig. 1c, ca. 2.5 ML) and below-monolayer loading (Fig. 1d, ca. 0.8 ML), but their density is considerably smaller in the latter. Chromia islands seem to grow on annealing (Fig. 1e).

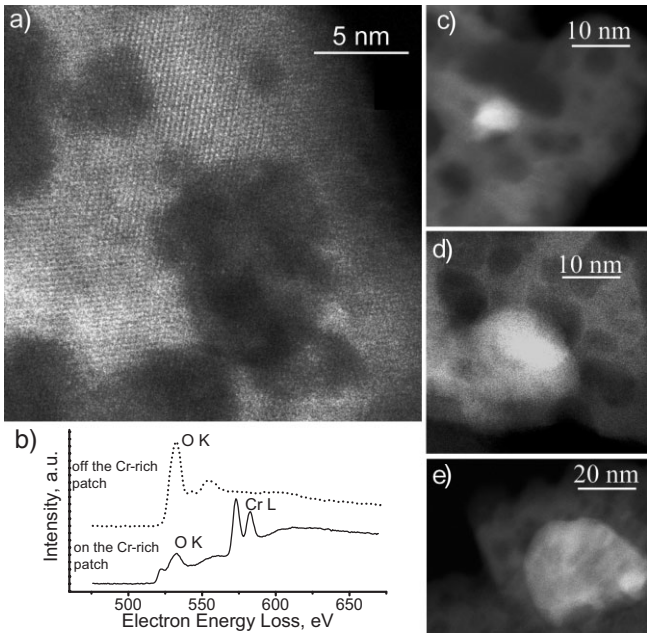

Figure 1. Cr-doped γ-Al_2O_3. a) STEM image (smoothed) of a γ-Al_2O_3 flake with Cr_2O_3 patches. b) EELS spectra, collected on the patches (dotted line) and between the patches (solid line), confirming Cr_2O_3 segregation. c–e) Chromia inclusions in an as-prepared sample with a loading of ca. 2.5 ML, an as-prepared sample with a loading of ca. 0.8 ML, and a sample with a loading of ca. 0.8 ML annealed at 600 °C for 24 h, respectively.

On η-Al_2O_3, on the other hand, no segregation was observed. Contrast in the STEM images of the sample with ca. 0.9 ML was mostly uniform, with the thinnest, off-axis areas of the alumina flakes sometimes displaying faint spots (indicated by the arrows in Fig. 2a). The EELS spectra, however, clearly showed the presence of Cr and no discernible difference in Cr concentrations between different areas of the sample (Fig. 2b). There was no apparent change in chromium distribution on annealing. A 2D Gaussian fit of the spots indicated by the arrows in Figure 2a shows that their incremental intensities are within 20 % of each other, and that the widths are 0.6–0.9 Å, which is about right for a single atom, in this case Cr. The signal-to-background ratios for the spots are fairly low, and while it is consistent with the moderate difference in atomic numbers between Cr and Al, the statistics of the *Z*-contrast images are insufficient proof for visualizing single Cr atoms. However, the combination with EELS data makes the achievement of such a visualization much more probable.

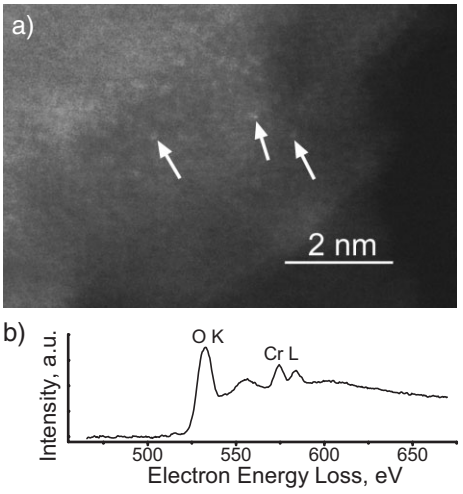

Figure 2. Cr-doped η-Al_2O_3. a) STEM image (smoothed) of an η-Al_2O_3 flake with possible single Cr atoms, indicated by the arrows. b) EELS spectrum, confirming the presence of Cr.

The EXAFS data provide further confirmation that the coordination environments of Cr in the two forms (γ- and η-Al_2O_3) are significantly different. A standard analysis of

 © 2007 WILEY-VCH Verlag GmbH & Co. KGaA, Weinheim

the X-ray absorption spectra gives the values of 5.8 and 4.5 (in γ- and η-alumina) for the coordination numbers of the Cr atoms in the first coordination spheres (Cr–O bonds), which corresponds to octahedral (characteristic of Cr^{3+}) and tetrahedral (characteristic of higher Cr oxidation states) coordination of Cr atoms in the two polytypes, respectively. The absence of any long-range order for Cr/η-Al_2O_3 suggests the existence of small monodisperse Cr clusters, while the Cr K-edge EXAFS signal from the γ-alumina surface ideally corresponds to the crystalline structure of Cr_2O_3 (Fig. 3).

To understand the difference in behavior of CrO_x clusters adsorbed on different transition aluminas, we performed extensive first-principles calculations to find the minimum-energy configurations of individual CrO_x ($x = 1$–4) clusters on the preferentially exposed η- and γ-Al_2O_3 (110C) surfaces (where C refers to having a topmost Al layer in which Al atoms have two different coordinations).[1,11] These surfaces are generally terminated by OH groups. We have considered CrO_x clusters either adsorbing on "bare" oxygen sites or replacing H atoms, for which calculations were carried out without H. Unlike the bare Cr atoms considered in previous work,[15] CrO_x clusters do not have a tendency to get buried under the surface of γ-Al_2O_3. The minimum-energy configurations for a CrO_3 cluster are shown in Figure 4. The bulk crystal structures of these two transition alumina polytypes are very similar: both are defect spinels in which 11 % of the cation sites are vacant to satisfy the Al_2O_3 stoichiometry. In γ-Al_2O_3 most of the vacancies are located in tetrahedral sites, whereas in η-Al_2O_3 they are distributed mainly in the octahedral sites.[10] This difference, however, results in sufficiently distinct diffraction patterns,[10] and significantly affects the surface relaxation processes in these polytypes, which results in their different surface reactivity.[11]

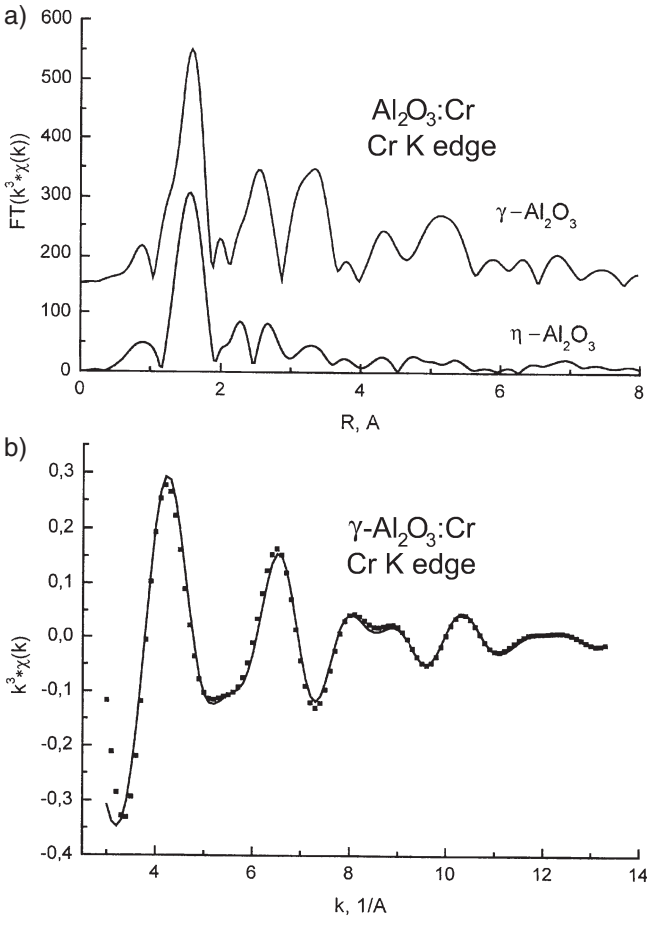

Figure 3. a) Fourier transforms of EXAFS spectra for Cr/γ-Al_2O_3 and Cr/η-Al_2O_3 catalytic couples (Cr K-edge). The absence of any well-defined structures in the second and higher coordination spheres for Cr/η-Al_2O_3 suggests the existence of small monodisperse Cr species at the η-Al_2O_3 surface. The presence of well-defined peaks in the higher-order coordination spheres for Cr/γ-Al_2O_3 confirms the presence of long-range ordering; b) The Cr K-edge EXAFS spectrum of Cr-doped γ-alumina (dots) gives a perfect fit with the crystalline structure of Cr_2O_3 (solid line), thus confirming the crystal structure of the Cr patches.

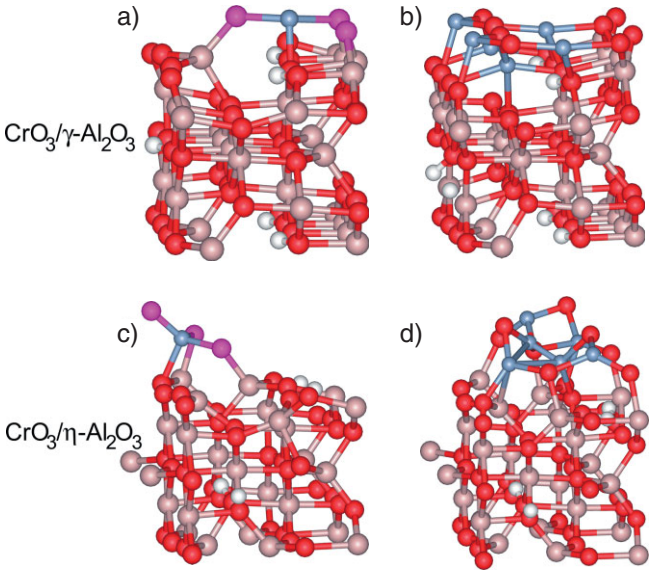

Figure 4. a,c) Schematics of the configurations for individual CrO_3 clusters positioned at the (100C) surface of γ-Al_2O_3 and η-Al_2O_3, respectively, determined by first-principles calculations. b,d) The relaxed structures, obtained by deposition of two regular Cr_2O_3 layers on γ-Al_2O_3 and η-Al_2O_3, respectively. The Al, O, H, and Cr atoms are shown in gray, red, white, and blue, respectively. The O atoms that belong to the CrO_3 clusters are shown in purple.

At the clean γ-Al_2O_3 (110C) surface, all of the oxygen atoms in the CrO_x clusters are found to be located at the sites that match well with the oxygen sublattice of γ-Al_2O_3 (Fig. 4a). In addition, the Cr atom binds to the surface oxygen atoms and occupies a site that corresponds to an octahedral site of bulk γ-Al_2O_3. Both of these facts suggest that nucleation of Cr_2O_3 on γ-Al_2O_3 does not introduce any significant strain at the interface, facilitating the growth of crystalline Cr_2O_3 particles where all the Cr atoms are octahedrally coordinated. As Figure 4b clearly demonstrates, Cr_2O_3 particles can grow in a commensurate way on a γ-Al_2O_3 surface. At low chromia loadings, however, the number of individual

© 2007 WILEY-VCH Verlag GmbH & Co. KGaA, Weinheim

ADVANCED MATERIALS

CrO_x clusters located at the surface may still be quite significant.

The η-alumina (110C) surface is markedly different from the corresponding γ-Al_2O_3 surface, as it contains unsaturated Al atoms with a coordination number of three.[14,15] The minimal energy for CrO_x clusters corresponds to the attachment of its oxygen atoms to these Al atoms. The two three-coordinated aluminum atoms that bond to the CrO_3 clusters are located in different rows (Fig. 4c). The resulting configuration shows a mismatch of the oxygen sites of the CrO_3 with the oxygen sublattice of the alumina substrate. In addition, the Cr atom in this configuration prefers tetrahedral coordination. As a result, nucleation of crystalline Cr_2O_3 particles on the η-alumina surface is unlikely (Fig. 4d). We conclude, therefore, that CrO_x clusters on the η-alumina surface remain dispersed.

We further used density functional calculations to explore the catalytic dehydrogenation of alkanes at the atomic level. As an example, Figure 5 shows the key step of the dehydrogenation of a C_2H_6 molecule at a CrO_3 cluster supported on the η-Al_2O_3 surface. When C_2H_6 approaches the CrO_3 cluster, two hydrogen atoms from the molecule get captured at the low-coordination oxygen sites and the remaining C_2H_4 molecule is released. This process entails an energy gain in the range of 1.3 to 1.6 eV, depending on which O sites the hydrogens are attached to, and on the value of x in CrO_x. The key enabler for the process is the low coordination of the O atoms on the CrO_x cluster. A flow of O_2 molecules is then necessary to remove the bound hydrogens and reactivate the site. The reaction $CrO_xH_2 + 1/2\,O_2 \rightarrow CrO_x + H_2O$ leads to a gain of energy in the range 0.7–0.9 eV, indicating that the hydrogens are removed in the form of water molecules.

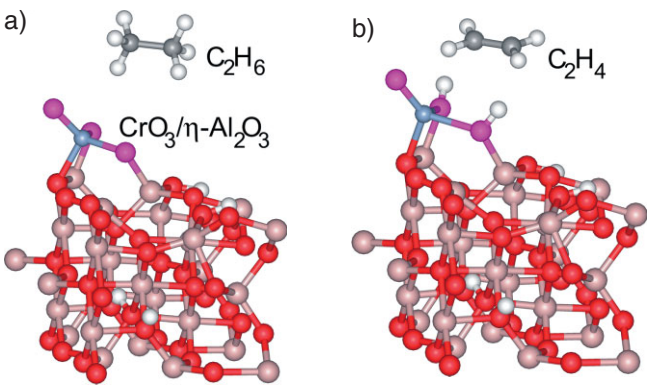

Figure 5. Dissociation of a C_2H_6 molecule on a CrO_3 cluster attached to a (110C) η-Al_2O_3 surface. a) Initial atomic configuration with a free alkane molecule (C_2H_6). b) Final configuration with a free alkene (C_2H_4) molecule and two H atoms captured and trapped at the active oxygen sites of the CrO_3 catalytic cluster.

The formed C_2H_4 molecule may either depart or bind to either the free alumina surface or to one of the CrO_x clusters, but in both cases the binding energy does not exceed 1.3 eV. Because typical temperatures for the dehydrogenation process are high (600–900 °C), the C_2H_4 molecule will not be trapped at the surface for long. Finally, we found that hydrogen atoms do not bind to the Cr atoms, as has been suggested previously.[9] Only the unsaturated oxygen atoms in the individual CrO_x cluster may capture and trap the H atoms from alkane molecules, in agreement with the conclusions of Chen et al. about the role of the VO_x/ZrO_2 catalyst in the oxidative dehydrogenation of propane.[7] It is also worth mentioning that the calculated difference in catalytic activity for isolated CrO_x on a γ-Al_2O_3 surface versus an η-Al_2O_3 surface is minimal. However, if the dispersed CrO_x clusters sinter and form larger clusters of chromium oxide (e.g., at higher chromium loadings or at higher temperatures) the oxygen atoms in crystalline Cr_2O_3 particles acquire higher coordination and become less active. If fact, we found that the dissociation of C_2H_6 on a crystalline Cr_2O_3 (0001) surface is energetically unfavorable, with an energy cost of ca. 2.8 eV (if the formed C_2H_4 molecule remains in the gas phase) or ca. 2.5 eV (if the dissociated C_2H_4 binds to the surface). This result explains why the catalytic activity decreases significantly when crystalline Cr_2O_3 is formed. Thus, only dispersed CrO_x clusters play a critical role in the catalytic reaction of the dissociation of alkanes.

In addition, CrO_x clusters may bond stably at surface steps or particle edges, where the catalytic reactions may be somewhat different. However, their role in catalysis would be secondary because they constitute a small fraction of the total catalyst surface.

It is also possible that Cr_nO_y species, where n = a small number (e.g., 2 or 3) also have low-coordination O atoms and would also, therefore, be catalytically active. Investigation of such possibilities represents one route towards optimized design of catalysts for specific applications.

In conclusion, we have investigated the Cr distribution in Cr/γ-Al_2O_3 and Cr/η-Al_2O_3 systems. *Z*-contrast STEM and EELS studies have demonstrated that while Cr is segregated into patches on γ-Al_2O_3 surface, it is distributed uniformly on η-Al_2O_3. EXAFS has identified the patches on γ-Al_2O_3 surface to be crystalline Cr_2O_3, while on η-Al_2O_3 the data analysis suggests small isolated CrO_x clusters with Cr coordination close to tetrahedral. First principles calculations trace this disparity back to the bulk structure of the respective alumina polymorphs and the resulting differences in the surface reconstruction: the reconstruction on γ-alumina facilitates the formation of crystalline Cr_2O_3 in registry with the substrate, while the reconstruction on η-alumina does not. The calculations further demonstrate that only the isolated CrO_x clusters are active in alkane dehydrogenation, with important implications for the longevity of catalysts.

Experimental

Samples for the study were fabricated at BASF Catalysts. To prepare Cr_2O_3/γ-Al_2O_3 (L6831-8-2) samples, boehmite alumina (Alcoa HiQ 180), nitric acid and water were blended, formed into cylindrical extrudates, dried at 120 °C overnight, and then calcined at 850 °C

 © 2007 WILEY-VCH Verlag GmbH & Co. KGaA, Weinheim

for 2 h. The extrudates were impregnated with chromic acid/sodium dichromate to incipient wetness, dried at 120 °C overnight, and calcined at 660 °C for 1 h. The samples with coverages of 2.5 ML and 0.8 ML were produced by varying the amount of Cr-containing reagent. To prepare $Cr_2O_3/\eta\text{-}Al_2O_3$ samples (L-6831-8-3), alumina extrudates (Al-5635, proprietary, BASF Catalysts alumina support) were calcined at 450 °C for 2 h, impregnated with chromic acid/sodium dichromate to incipient wetness, dried at 120 °C overnight, and then calcined at 660 °C for 1 h to produce a catalyst with 0.9 ML coverage. For microscopic observations, extrudate particles were crushed and deposited onto holey carbon grids. Both as-prepared samples and samples annealed at 600 °C for 48 h were examined. While annealing did not duplicate the conditions inside the reactor, it served as a test for the thermal stability of the dopant distribution in as-prepared samples.

Z-contrast STEM observations were carried out with a VG Microscopes HB603U instrument, operated at 300 kV and equipped with Nion aberration corrector to give sub-Ångstrom probe size [16] and superior signal-to-noise ratio. EELS spectra were collected by using a VG Microscopes HB501UX microscope operated at 100 kV and equipped with a McMullan design charge-coupled device (CCD) parallel detection EELS system [17].

EXAFS measurements were performed in the regime of total external reflection at room temperature at the Institute of Nuclear Physics of the Russian Academy of Sciences (the Novosibirsk Center for Synchrotron Radiation). Synchrotron radiation was properly preconditioned by using the Si (111) monochromator.

The first-principles calculations (spin-polarized) were performed within density functional theory, using the pseudopotential method and a plane wave basis set [15,18,19]. The exchange-correlation effects were treated with the generalized gradient-corrected exchange-correlation functionals (GGA) given by Perdew and Becke [20]. We adopted a norm-conserving pseudopotential for Al and the Vanderbilt ultrasoft pseudopotentials for Cr, O, and H atoms [18,21]. A plane wave energy cutoff of 400 eV and two special $\boldsymbol{k}$ points in the irreducible part of the 2D Brillouin zone of the surfaces were used for calculating the preferentially exposed (110C) surfaces of γ- and $\eta\text{-}Al_2O_3$ [14]. Semi-infinite (110C) surfaces were modeled by repeated slabs (supercells) containing 5–8 layers (70–128 atoms per supercell, respectively) separated by a vacuum region equivalent to 10–12 Å. Supercells containing 80 atoms and a 2×2 surface cell were employed to represent the $\alpha\text{-}Cr_2O_3(0001)$ surface. The cation vacancies that are inherently present in the spinel form of $\gamma\text{-}Al_2O_3$ and $\eta\text{-}Al_2O_3$ were located on the tetrahedral and octahedral cation sublattices, respectively. All the atoms in the supercell, except for those in the lower two or three atomic layers (which were kept fixed), were relaxed until the forces on the atoms were smaller than 0.05 eV $Å^{-1}$. CrO_x ($x = 1$–4) species with different initial geometries on both γ- and $\eta\text{-}Al_2O_3$ (110C) surfaces were examined to find the minimum-energy configurations. For each configuration, various combinations of O sites for H attachment were examined to obtain the reaction energies for dehydrogenation of a C_2H_6 molecule on CrO_x clusters, crystalline Cr_2O_3, and transition aluminas.

Received: July 19, 2006
Revised: January 18, 2007
Published online: July 12, 2007

[1] H. Knozinger, P. Ratnasamy, *Catal. Rev. Sci. Eng.* **1978**, *17*, 31.
[2] a) C. N. Satterfield, *Heterogeneous Catalysis in Practice*, McGraw-Hill, New York **1980**. b) M. F. M. Zwinkels, S. G. Jaras, P. G. Menon, T. A. Griffin, *Catal. Rev. Sci. Eng.* **1993**, *35*, 319.
[3] M. Cherian, M. S. Rao, W. T. Yang, H. M. Jehng, A. M. Hirt, G. Deo, *Appl. Catal., A* **2002**, *233*, 21.
[4] D. W. Flick, M. C. Huff, *Appl. Catal., A* **1999**, *187*, 13.
[5] P. W. Park, J. S. Ledford, *Langmuir* **1997**, *13*, 2726.
[6] a) E. Garrone, G. Ghiotti, S. Coluccia, A. Zecchina, *J. Phys. Chem.* **1975**, *79*, 984. b) D. S. Kim, I. E. Wachs, *J. Catal.* **1993**, *142*, 166. c) M. Hoang, J. F. Mathews, K. C. Pratt, *React. Kinet. Catal. Lett.* **1997**, *61*, 21. d) M. I. Zaki, N. E. Fouad, J. Leyrer, H. Knozinger, *Appl. Catal.* **1986**, *21*, 359. e) H. H. Kung, *Adv. Catal.* **1994**, *40*, 1. f) D. Creaser, B. Andersson, *Appl. Catal., A* **1996**, *141*, 131.
[7] K. D. Chen, A. T. Bell, E. Iglesia, *J. Phys. Chem. B* **2000**, *104*, 1292.
[8] a) S. De Rossi, G. Ferraris, S. Fremiotti, E. Garrone, G. Ghiotti, M. C. Campa, V. Indovina, *J. Catal.* **1994**, *148*, 36. b) K. Jagannathan, A. Srinivasan, C. N. R. Rao, *J. Catal.* **1981**, *69*, 418. c) A. Ellison, *J. Chem. Soc., Faraday Trans. 1* **1984**, 2567. d) W. Grünert, E. S. Shpiro, R. Feldhaus, K. Anders, G. V. Antoshin, K. M. Minachev, *J. Catal.* **1986**, *100*, 138, e) A. M. Turek, I. E. Wachs, E. Decanio, *J. Phys. Chem.* **1992**, *96*, 5000. f) B. M. Weckhuysen, R. A. Schoonheydt, J. M. Jehng, I. E. Wachs, S. J. Cho, R. Ryoo, S. Kijlstra, E. Poels, *J. Chem. Soc., Faraday Trans.* **1995**, 3245. g) B. M. Weckhuysen, I. E. Wachs, R. A. Schoonheydt, *Chem. Rev.* **1996**, *96*, 3327.
[9] B. M. Weckhuysen, R. A. Schoonheydt, *Catal. Today* **1999**, *51*, 223.
[10] R.-S. Zhou, R. L. Snyder, *Acta Crystallogr., Sect. B* **1991**, *47*, 617.
[11] K. Sohlberg, S. J. Pennycook, S. T. Pantelides, *J. Am. Chem. Soc.* **1999**, *121*, 7493.
[12] S. Alerasool, personal communication.
[13] S. Alerasool, H. E. Manning, *US Patent 7 012 038*, **2006**.
[14] K. Sohlberg, S. T. Pantelides, S. J. Pennycook, *J. Am. Chem. Soc.* **2001**, *123*, 26.
[15] S. N. Rashkeev, K. Sohlberg, M. V. Glazoff, J. Novak, S. J. Pennycook, S. T. Pantelides, *Phys. Rev. B* **2003**, *67*, 115 414.
[16] P. D. Nellist, M. F. Chisholm, N. Dellby, O. L. Krivanek, M. F. Murfitt, Z. S. Szilagyi, A. R. Lupini, A. Borisevich, W. H. Sides, S. J. Pennycook, *Science* **2004**, *305*, 1741.
[17] D. McMullan, J. M. Rodenburg, Y. Murooka, A. J. McGibbon, *Inst. Phys. Conf. Ser.* **1990**, 55.
[18] G. Kresse, J. Furthmuller, *Comput. Mater. Sci.* **1996**, *6*, 15.
[19] S. W. Wang, A. Y. Borisevich, S. N. Rashkeev, M. V. Glazoff, K. Sohlberg, S. J. Pennycook, S. T. Pantelides, *Nat. Mater.* **2004**, *3*, 143.
[20] a) J. P. Perdew, *Phys. Rev. B* **1986**, *33*, 8822. b) A. D. Becke, *Phys. Rev. A* **1988**, *38*, 3098.
[21] D. Vanderbilt, *Phys. Rev. B* **1990**, *41*, 7892.

© 2007 WILEY-VCH Verlag GmbH & Co. KGaA, Weinheim